Asian Journal of Pharmaceutical Sciences 13 (2018) 498–504

Available online at www.sciencedirect.com

ScienceDirect

journal homepage: www.elsevier.com/locate/AJPS

Original Research Papers

Preparation and characterization of nanoparticles from quaternized cyclodextrin-grafted chitosan associated with hyaluronic acid for cosmetics

Sakhiran Sakulwech[a], *Nattaya Lourith*[a,b], *Uracha Ruktanonchai*[c], *Mayuree Kanlayavattanakul*[a,b,*]

[a] *School of Cosmetic Science, Mae Fah Luang University, Chiang Rai 57100, Thailand*
[b] *Phytocosmetics and Cosmeceuticals Research Group, Mae Fah Luang University, Chiang Rai 57100, Thailand*
[c] *National Nanotechnology Center, National Science and Technology Development Agency, Pathum Thani 12120, Thailand*

ARTICLE INFO

Article history:
Received 31 October 2017
Revised 18 April 2018
Accepted 18 May 2018
Available online 15 June 2018

Keywords:
Hyaluronic acid
QCD-g-CS
Polymeric nanoparticles
Ionic gelation
Delivery system

ABSTRACT

Hyaluronic acid (HA, 20–50 kDa) is a hydrophilic macromolecule with anti-wrinkle effects and moisturizing properties. However, its high molecular weight prevents it from penetrating into the deeper layers of the skin and, thus, limits its benefits to topical effects. Thus, the objective of this study is to prepare nanoparticles of quaternized cyclodextrin-grafted chitosan (QCD-g-CS) associated with HA in different molar ratios of QCD-g-CS and HA. The conjugation of the carboxylic moieties of HA and the amides of QCD-g-CS was confirmed by Fourier-transform infrared spectroscopy. Thus, the system was optimized to create nanoparticles with a small size (235.63 ± 21.89 nm), narrow polydispersity index (0.13 ± 0.02), and zeta potential of 16.07 ± 0.65 mV. The association efficiency and loading efficiency were determined by ultra-performance liquid chromatography as 86.77 ± 0.69% and 10.85 ± 0.09%, respectively. The spherical morphology of the obtained nanoparticles was confirmed by transmission electron microscopy. Moreover, the *in-vitro* hydrating ability was significantly higher ($P < 0.001$) than that of bulk HA (3.29 ± 0.41 and 1.71 ± 0.05 g water/g sample, respectively). The safety of these nanoparticles at concentrations in the range of 0.01–0.10 mg/ml was confirmed via tests on human skin fibroblasts. Together, these results demonstrate that the developed nanoparticles are promising for future applications in cosmetics.

© 2018 Shenyang Pharmaceutical University. Published by Elsevier B.V.
This is an open access article under the CC BY-NC-ND license.
(http://creativecommons.org/licenses/by-nc-nd/4.0/)

* Corresponding author. School of Cosmetic Science, Mae Fah Luang University, Chiang Rai 57100, Thailand. Tel.: +6653916832.
E-mail address: mayuree@mfu.ac.th (M. Kanlayavattanakul).
Peer review under responsibility of Shenyang Pharmaceutical University.

https://doi.org/10.1016/j.ajps.2018.05.006
1818-0876/© 2018 Shenyang Pharmaceutical University. Published by Elsevier B.V. This is an open access article under the CC BY-NC-ND license. (http://creativecommons.org/licenses/by-nc-nd/4.0/)

1. Introduction

β-cyclodextrin (β-CD) and chitosan (CS) are popular biopolymers for drug-delivery systems: the β-CD can enhance the solubility, dissolution rate, bioavailability, stability, and controlled release of a hydrophobic guest molecule while CS is a positively charged biopolymer with non-toxic, biodegradable, antimicrobial, and mucoadhesive properties [1,2]. To leverage the beneficial properties of both of these biopolymers, Venter et al. synthesized cyclodextrin-grafted chitosan (CD-g-CS) [3]. However, as the synthesized CD-g-CS has poor stability in water, Gonil et al. modified the CD-g-CS by means of quaternization to obtain water-soluble quaternized cyclodextrin-grafted chitosan (QCD-g-CS) [4]. A QCD-g-CS composition of 11% cyclodextrin grafted on chitosan was found to yield the highest degree of quaternization of 73% ± 2% with a molecular weight of 81.24 kDa and provided the best mucoadhesive ability, drug entrapment capacity, and antimicrobial properties [5]. In a previous study [2,6], the ability of QCD-g-CS to entrap hydrophobic guest molecules like menthol and eugenol was investigated. However, QCD-g-CS retained its positive charge and, thus, would be unable to carry a negatively charged drug molecule.

Hyaluronic acid (HA) is a hydrophilic, negatively charged linear polysaccharide composed of alternating D-glucuronic acid (GlcUA) and *N*-acetyl- D-glucosamine (GlcNAc) units [7]. HA is popular in medical applications for treating osteoarthritis, embryo implantation, and cutaneous wound healing. Moreover, HA has been used in dermatological and cosmetic products to improve skin elasticity, turgor, and moisture [8,9]. HA is a major extracellular matrix component and acts as a sponge in the skin to retain water and provide elasticity. However, the benefits of HA are limited due to its large molecular weight, which prevents skin penetration [10]. HA can be hydrolyzed to have a molecular weight of 20–50 kDa to promote skin penetration and provide anti-wrinkle and moisturizing effects [11]. Therefore, HA is an excellent candidate as a negatively charged macromolecule with versatile functions to incorporate with QCD-g-CS.

In this study, we aim to produce nanoparticles of QCD-g-CS associated with HA (20–50 kDa). Several physicochemical characteristics of the nanoparticles are characterized: particle size, zeta potential, polydispersity index (Pdi), association efficacy, loading efficacy, structural confirmation, morphology, water retention capacity, and safety. The developed system will enable effective delivery of HA to the deeper layers of the skin to enhance its moisturizing effects.

2. Materials and methods

2.1. Materials

Cosmetic grade sodium hyaluronate with molecular of 20–50 kDa was purchased from Givaudan (Vernier, Switzerland). QCD-g-CS was synthesized by the method of Gonil and coworker at the National Nanotechnology Center (NANOTEC) (Pathumthani, Thailand) as per we had reported [3–5]. Sodium hydroxide (NaOH) and disodium hydrogen phosphate (Na_2HPO_4) were of analytical grade supplied from Merck (New Jersey, USA). The deionized (DI) water was produced from a Milli-Q water purification system (Millipore, Massachusetts, USA). Human skin fibroblasts (ATCC® CRL 2097, USA) at 14–20th passage were used for cytotoxicity assessment. Dulbecco's Modified Eagle's Medium (DMEM), Fetal Bovine Serum (FBS), penicillin and streptomycin were from Gibco (New Hampshire, USA). Trypsin and sulforhodamine B dye were obtained from Sigma-Aldrich (Missouri, USA).

2.2. Methods

2.2.1. Preparation of QCD-g-CS associated HA nanoparticles

QCD-g-CS and HA (20–50 kDa) were separately dissolved in DI water at 2 mg/ml. The HA solution was ultra-sonicated (Sonics VCX-130 PB Vibra cell™, Connecticut, USA) for 3 min. The HA nanoparticles were prepared by slow addition of HA solution into QCD-g-CS solution as different mole ratio (0.3–2 mol) with stirring [12].

2.2.2. Determination of particle size, zeta potential and polydispersity index (PDI) of QCD-g-CS associated HA nanoparticles

HA nanoparticles were analyzed with zetasizer® (NanoZS4700 nanoseries, Malvern, UK). at 25 °C [6].

2.2.3. Determination of the loading efficiency and association efficiency by ultra-performance liquid chromatography

Each prepared HA nanoparticles were centrifuged (Kubota, Osaka, Japan) to separate pellets, and pellets were freeze-dried. These nanoparticles were resuspended in phosphate buffer, and ultrasonicated. The dialysates were filtered (0.4 µm) further to UPLC analysis (Waters Acquity H-Class system, Acquity UPLC PDA eλ detector, BEH C18 1.7 mm column (2.1 mm × 100 mm, Waters, Massachusetts, USA)) with the isocratic mobile phase of potassium dihydrogen phosphate buffer (0.05 M, pH 7.0). The analytical condition was optimized and validated at the flow rate of 0.4 ml/minutes with the injection volume of 10 µL and the column was set at 25 °C with the analytical time last for 1.5 min [13]. The percentage of loading efficiency can be calculated according to the following equations [1].

$$\text{Loading\%} = \frac{\text{Detected amount of HA}}{\text{Weight of freeze dry pellets}} \times 100$$

$$\text{AE\%} = \frac{\text{Detected amount of HA}}{\text{Initial HA added}} \times 100$$

2.2.4. Structural confirmation of QCD-g-CS associated HA nanoparticles with FTIR

The QCD-g-CS, HA, and the selected dried HA nanoparticles were FTIR analyzed (Perkin Elmer Spectrum-GX FT-IR spectrometer, Massachusetts, USA). The spectra were from 4000 to 400 cm^{-1} [1].

2.2.5. Morphological observations

The QCD-g-CS, HA, and the selected HA nanoparticles were dropped on the carbon-coated copper grid and stained by phosphotungstic acid (1%, w/v) or uranyl acetate (2%, w/v), and observed by transmission electron microscopy (TEM, JEOL JEM-2010, Tokyo, Japan) at 120 kV [1].

2.2.6. Determination of the water retention capacity

The QCD-g-CS, HA and the selected HA nanoparticles were hydrated for 30 min and centrifuged (Hettich® Universal 320R, Tuttlingen, Germany). The supernatant was decanted and the residue hydrated weight was recorded. The result was expressed as the amount of water retained by the pellet (water/dried sample, g/g) [14].

2.2.7. Assessment of the cytotoxicity on human skin fibroblasts

Fibroblast cells were cultured in 75 cm^2 flask with DMEM medium contained 10%FBS and 1%penicillin/streptomycin. Cultured cells are incubated at 37 °C in a humidified incubator with 5% CO_2. QCD-g-CS, HA, and the selected HA nanoparticles were evaluated for cytotoxicity using Sulforhodamine B (SRB) assay [15]. The absorbance was recorded using a microplate reader (SPECTROstar Nano, BMG Labtech, Germany).

2.2.8. Statistical analyses

Experimental results are given as mean ± standard deviation. Analysis of variance and least significant different test by using ANOVA test were done with statistic program SPSS version 21.0. The level of significance was at $P < 0.05$.

3. Results and discussion

A previous study demonstrated the ability of QCD-g-CS to entrap hydrophobic guest molecules within cyclodextrin cavities to improve the drug solubility and mucoadhesivity [2]. However, there remains potential to bond the amide groups of the chitosan to a negatively charged molecule such as HA. Thus, QCD-g-CS-associated HA nanoparticles were prepared and characterized herein in an attempt to widen its applications in cosmetics.

3.1. Preparation and characterization of QCD-g-CS-associated HA nanoparticles

Nanoparticles composed of HA were prepared by the ionotropic gelation technique. The ability of CS to form a gel upon contact with HA, which is a polyanionic molecule, by forming inter- and intramolecular linkages to form nanoparticles [16]. This ionic gelation process is simple, involving the mixing of two aqueous phases at room temperature. The HA nanoparticles were prepared with a range of molar ratios as shown in Fig. 1.

Increasing the HA content resulted in the formation of larger nanoparticles with lower zeta potentials due to the negative charge of the HA. The low-zeta-potential nanoparticles can form aggregates and precipitates via low electrostatic repulsion, resulting in high particle sizes and Pdi [17] for HA0.8_NPs, HA1.0_NPs, HA1.5_NPs, and HA2.0_NPs. The zeta potential of HA0.8_NPs and HA1.0_NPs was 0 mV (isoelectric), leading to precipitation. The HA0.3_NPs were the smallest in size (20–600 nm), thus promoting skin penetration via skin furrows and follicles, and had a narrow Pdi and high zeta potential, making them stable due to the strong electrostatic repulsion barrier [18,19].

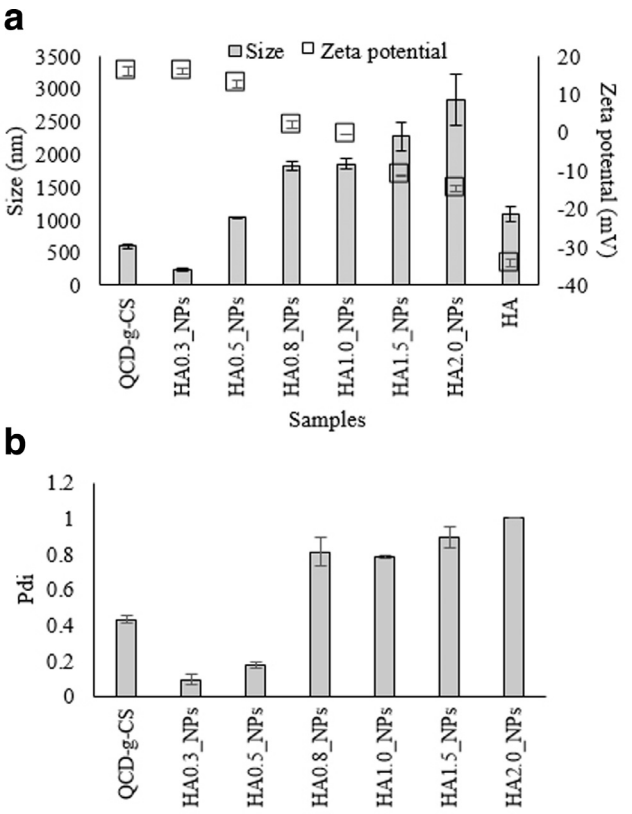

Fig. 1 – The particle size and zeta potential (a) and the polydispersity index (b) of each sample.

3.2. Determination of the loading efficiency and association efficiency by ultra-performance liquid chromatography

The association efficiency (AE%) was defined as the percentage of HA that was successfully associated with nanoparticles. The loading efficiency (loading%) was calculated as the total amount of associated HA divided by the total nanoparticle weight and represents the amount of drug delivered per unit weight of the nanoparticles [2].

Increasing the relative amount of HA decreased the AE% due to excess amount of HA that could not bind with QCD-g-CS and, thus, was lost during centrifugation (Fig. 2). The HA0.3_NPs had significantly higher %AE values ($P < 0.001$). On the contrary, increasing the relative amount of HA increased the loading%. The loading% values of the HA0.8_NPs, HA1.0_NPs, HA1.5_NPs, and HA2.0_NPs ranged from 10.85 to 14.86% but the differences were not statistically significant.

The changes in the AE% and loading% values of these nanoparticles were consistent with those reported in a previous study, which reported that more eugenol and menthol (0–20 mol) than HA (0–2 mol) were entrapped by QCD-g-CS [1] due to the different entrapment or association sites. As HA has a higher molecular weight and is more hydrophilic, it is not entrapped within the hydrophobic cyclodextrin cavity or the hydrophobic core of QCD-g-CS unlike eugenol and menthol [1,7,20]. HA does not spontaneously bond with cyclodextrin without chemical modification

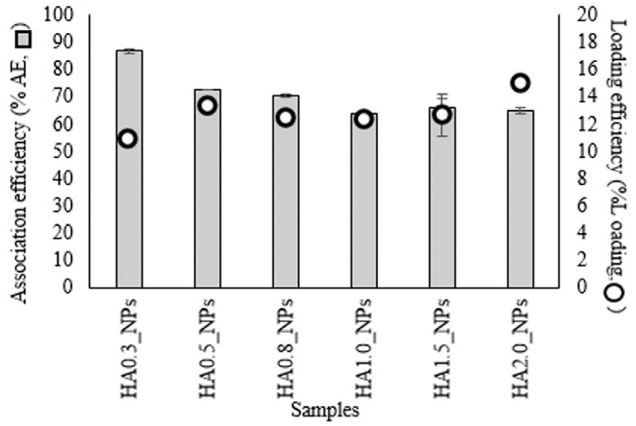

Fig. 2 – Association efficiency and loading efficiency of each sample.

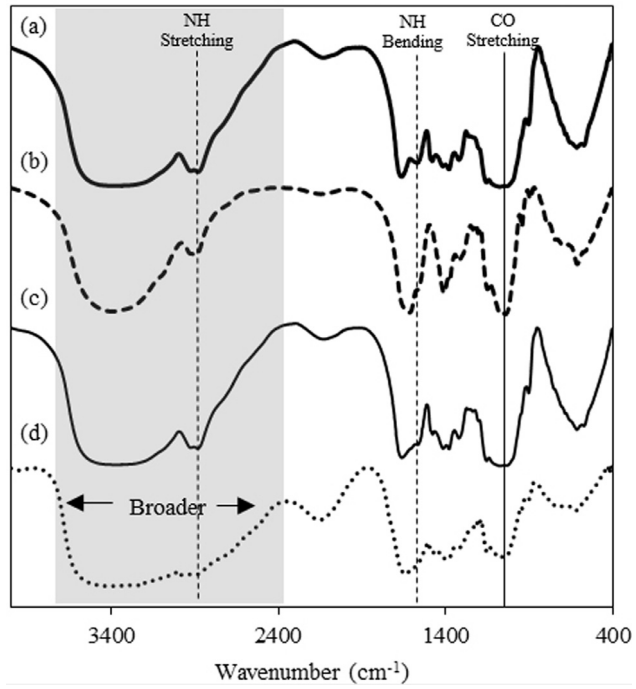

Fig. 3 – FTIR spectra of (a) QCD-g-CS, (b) HA, (c) a physical mixture of QCD-g-CS and HA and (d) HA0.3_NPs.

[21–23]. Therefore, HA should bond with the chitosan moieties of QCD-g-CS based on previous evidence supporting the complexation of chitosan and HA [16,24]. Thus HA0.3_NPs, the smallest of the nanoparticles formed, were selected for further assessment.

3.3. *Structural confirmation of QCD-g-CS associated HA nanoparticles with FTIR*

The FTIR spectra of QCD-g-CS, HA, an equimolar physical mixture of QCD-g-CS and HA, and HA0.3_NPs were obtained to confirm the bonding between HA and QCD-g-CS (Fig. 3). The spectrum of QCD-g-CS exhibited peaks at 1650 and 1560 cm^{-1}, indicating N–H bending within the primary and secondary amide groups, respectively. In addition, the N–H stretching at 2860 cm^{-1} confirmed the presence of these amide groups [11]. The FTIR spectrum of HA exhibited sharp asymmetric stretching at 1603 cm^{-1}, which is indicative of a carbonyl group within a glucuronic unit, overlapping peaks from 1475 to 1680 cm^{-1} corresponding to amide groups, and a Na-O peak at 823 cm^{-1} that is specific to sodium hyaluronate [25]. The HA and chitosan were conjugated to the carboxylic groups of HA and the amides of chitosan, which is consistent with the results of the previous study [25].

According to the spectra and structures of QCD-g-CS and HA (Fig. 5), HA can associate with QCD-g-CS by electrostatic interactions between the amide groups on chitosan (1560 and 2860 cm^{-1}) and the carboxylic group of HA (1060 cm^{-1}), resulting in disappearing or weakening of the signals of both functional groups as in the HA0.3_NPs spectrum. Moreover, the O–H and N–H peak (2350–3770 cm^{-1}) of HA0.3_NPs became broader due to the ionic absorption. The FTIR spectra also confirmed that nanoparticles were not formed by simple physical mixing and HA could not be incorporated into the cyclodextrin moieties due to the remaining characteristic peaks of HA. The inclusion complex of QCD-g-CS was observed as the disappearance of the characteristic peaks of the entrapped molecules [6,8]. The nanoparticles may have taken on condensed spherical shapes because the carboxylic groups on the HA bound to the amide groups that surrounded QCD-g-CS micelles.

3.4. *Morphological observations*

The shapes of the nanoparticles were further confirmed by transmission electron microscopy (TEM) as shown in Fig. 4. The HA0.3_NPs were spherical with diameters of 189 ± 10.02 nm, indicating that they were smaller than the particles formed in an aqueous environment using dynamic light scattering (DLS) (235.63 ± 21.89 nm). It should be noted that the DLS measurements gave the particle size including the hydrated shell surrounding the nanoparticle while TEM revealed the diameter of a dry nanoparticle i.e. the real size of a nanoparticle [6]. The QCD-g-CS was also spherical due to the formation of micelles composing the inner hydrophobic cyclodextrin cores and the outer hydrophilic chitosan regions [6]. The HA image demonstrated that HA had a globular form. Normally, HA is a linear chain polymer that can twist into a fibrillary aggregate form and contract into the globular form [26].

These results indicated that the selected nanoparticles were formed by an interaction between the HA chain and chitosan backbone of QCD-g-CS on the outer surface of the QCD-g-CS via electrostatic interactions [27]. Finally, HA bonded to the QCD-g-CS surface, resulting in a condensed spherical form with a hydrophobic cyclodextrin core as shown in Fig. 5. The FTIR spectra supported the occurrence of electrostatic interactions between the carboxylic groups on the HA chains and the amide groups on the chitosan backbone.

3.5. *Determination of the water retention capacity*

The water retention capacity (WRC) represents the ability of a sample to retain water after centrifugation and is used to assess the *in-vitro* moisturizing capability of a material [14].

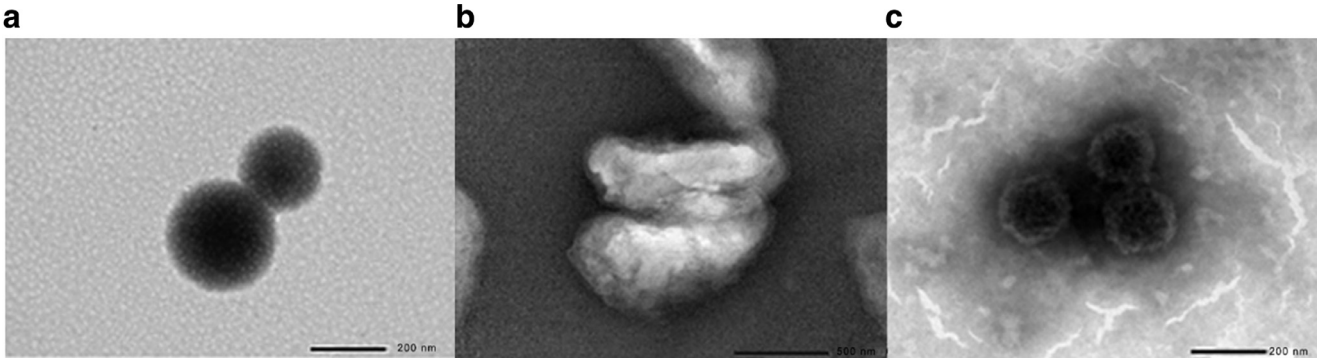

Fig. 4 – TEM image of (a) QCD-g-CS, (b) HA and (c) HA0.3_NPs.

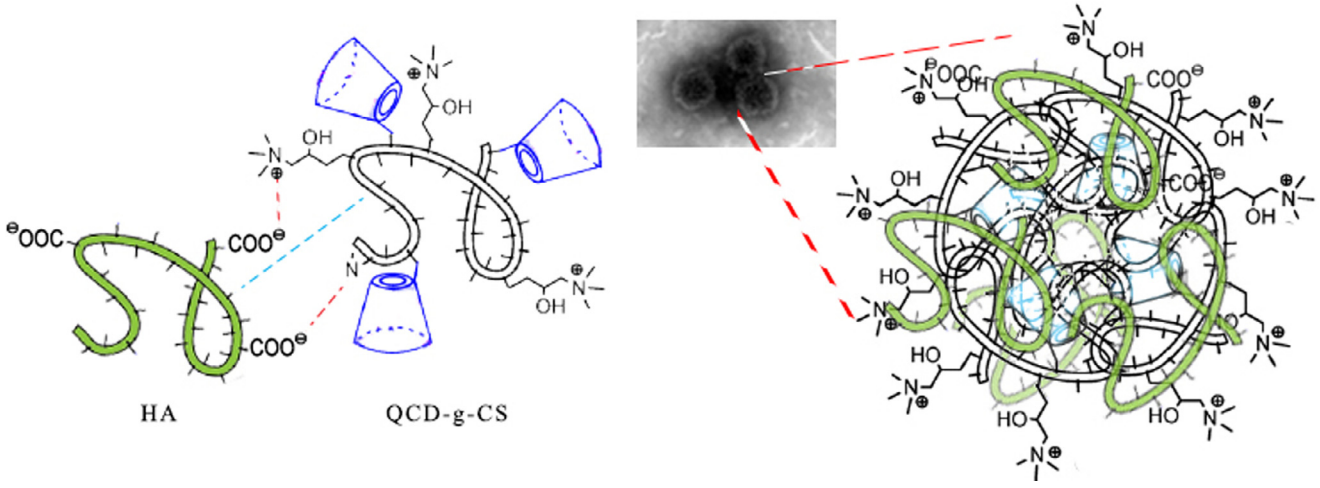

Fig. 5 – Schematic structure of HA with QCD-g-CS nanoparticles with TEM image of HA0.3_NPs.

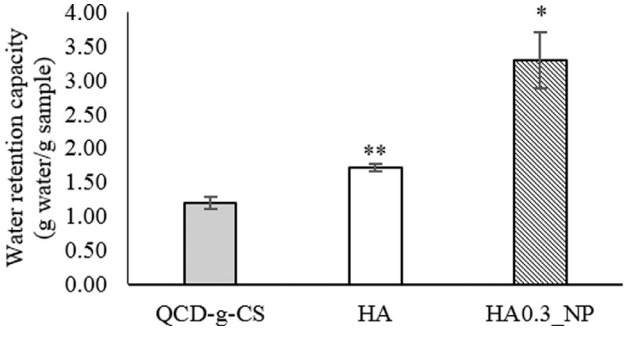

Fig. 6 – Water retention capacity of QCD-g-CS, HA, and HA0.3_NPs. (*: $P < 0.001$, **: $P = 0.001$).

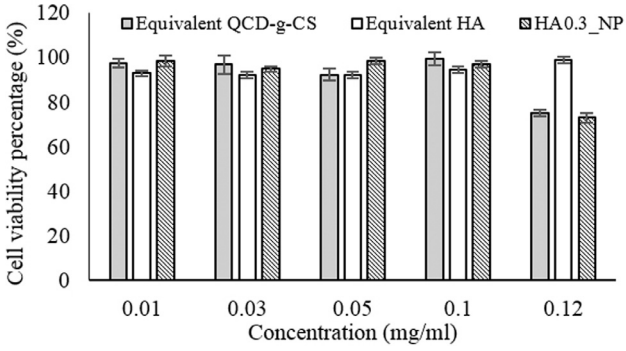

Fig. 7 – Cytotoxicity of QCD-g-CS, HA, and HA0.3_NPs towards human skin fibroblasts.

The WRC values of QCD-g-CS, HA, and HA0.3_NPs are shown in Fig. 6. The WRC of HA was significantly greater than that of QCD-g-CS ($P < 0.05$) due to the numerous glucuronic units in the HA as indicated by the sharp carbonyl FTIR peaks, indicating a hygroscopic effect [28]. The selected HA0.3_NPs exhibited a higher WRC value ($P < 0.05$) than HA and QCD-g-CS. HA and QCD-g-CS formed cross-linked networks to improve the WRC [29], which is expected to enhance the skin hydration effect [6]. However, prior to efficacy evaluation, an *ex-vivo* safety assessment is needed to guarantee the potential application of this material in cosmetics.

3.6. *Assessment of the cytotoxicity on human skin fibroblasts*

The safety of the nanoparticles for healthcare applications, including their use in cosmetics, necessitates a toxicity test

in mammalian cells [30]. The non-cytotoxicities of QCD-g-CS, HA, and HA0.3_NPs were verified at concentrations of 0.01–0.1 mg/ml by cell viabilities of more than 80% (Fig. 7). The HA was found to be safe but the QCD-g-CS and HA0.3_NPs were slightly cytotoxic at 0.12 mg/ml. Positively charged compounds can adhere to the cell membrane, thereby, and disrupt the cell [31]. The HA0.3_NPs exhibited a positive charge similar to that of QCD-g-CS due to the relatively high proportion of QCD-g-CS. HA is generally biocompatibility and non-toxic [7] but, when associated with QCD-g-CS, was cytotoxic at 0.12 mg/ml likely QCD-g-CS due to its similar positive zeta potential. The safety range of HA0.3_NPs was found to be 0.01–0.1 mg/ml.

4. Conclusion

In this study, the QCD-g-CS associated with HA nanoparticles were successfully formulated. HA0.3_NPs was the best formulation and provided desirable properties including a small particle size, a high zeta potential, and a narrow Pdi. The increasing HA ratio resulted in nanoparticles with increasing particles sizes, decreasing zeta potentials, increasing AE% values, and decreasing loading% values. The AE% and loading% values of the nanoparticles were shown to be 86.77% ± 0.69% and 10.85% ± 0.09%, respectively. The electrostatic interaction between QCD-g-CS and HA was confirmed by FTIR, suggesting that the nanoparticles were not formed by simple physical mixing. The WRC of the selected nanoparticles was improved due to the formation of cross-linked networks in the nanoparticles, improving their moisturizing efficacy. These nanoparticles were found to be safe at concentrations in the range of 0.01–0.1 mg/ml.

These results proved that QCD-g-CS is a versatile carrier for both negatively charged hydrophilic molecules and for hydrophobic drugs as reported previously. The development of these nanoparticles will be continued in a future study to investigate the factors influencing the skin penetration and evaluate the *in-vivo* efficacy for applications in cosmetics.

Conflicts of interest

The authors declare that there is no conflicts of interest.

Acknowledgments

Mae Fah Luang University is acknowledged for facilities and financially supported in part. National Nanotechnology Center (NANOTEC) is acknowledged for facilities supported. This study was funded by Thailand Graduate Institute of Science and Technology (TGIST), National Science and Technology Development Agency (NSTDA), Thailand (Project No. SCA-CO-2558-1026-TH). Dr. Puxvadee Chaikul is acknowledged for suggestion about cell culture study.

Supplementary materials

Supplementary material associated with this article can be found, in the online version, at doi:10.1016/j.ajps.2018.05.006.

REFERENCES

[1] Ikinci G, Şenel S, Akıncıbay H, et al. Effect of chitosan on a periodontal pathogen Porphyromonas gingivalis. Int J Pharm 2002;235:121–7.
[2] Phunpee S, Saesoo S, Sramala I, et al. A comparison of eugenol and menthol on encapsulation characteristics with water-soluble quaternized β-cyclodextrin grafted chitosan. Int J Biol Macromol 2016;84:472–80.
[3] Venter JP, Kotze AF, Auzely-Velty R, Rinaudo M. Synthesis and evaluation of the mucoadhesivity of a CD-chitosan derivative. Int J Pharm 2006;313:36–42.
[4] Gonil P, Sajomsang W, Ruktanonchai UR, et al. Novel quaternized chitosan containing β-cyclodextrin moiety: Synthesis, characterization and antimicrobial activity. Carbohydr Polym 2011;83:905–13.
[5] Sajomsang W, Gonil P, Ruktanonchai UR, et al. Self-aggregates formation and mucoadhesive property of water-soluble β-cyclodextrin grafted with chitosan. Int J Biol Macromol 2011;48:589–95.
[6] Sajomsang W, Nuchuchua O, Gonil P, et al. Water-soluble β-cyclodextrin grafted with chitosan and its inclusion complex as a mucoadhesive eugenol carrier. Carbohydr Polym 2012;89:623–31.
[7] Brown MB, Jones SA. Hyaluronic acid: a unique topical vehicle for the localized delivery of drugs to the skin. J Eur Acad Dermatol Venereol 2005;19:308–18.
[8] Chen M, Gupta V, Anselmo AC, Muraski JA, Mitragotri S. Topical delivery of hyaluronic acid into skin using SPACE-peptide carriers. J Control Release 2014;173:67–74.
[9] Mero A, Campisi M. Hyaluronic acid bioconjugates for the delivery of bioactive molecules. Polymers 2014;6:346–69.
[10] Olejnik A, Goscianska J, Zielinska A, Nowak I. Stability determination of the formulations containing hyaluronic acid. Int J Cosmet Sci 2015;37:401–7.
[11] Farwick M, Lersch P, Strutz G. Low molecular weight hyaluronic acid: its effects on epidermal gene expression & skin aging. SÖFW J 2008;134:1–6.
[12] Saengsitthisak B. Epigallocatechin gallate loaded chitosan nanoparticles. Chiang Mai: Chiang Mai University; 2007. Master [Thesis] Available from: Thai Library Integrated System.
[13] Sakulwech S, Kanlayavattanakul M, Lourith N, Ruktanonchai U. Validated determination of hyaluronic acid by UPLC-UV for pharmaceutical products. In: Proceedings of PACCON 2017; 2017 Feb 2-3; Bangkok, Thailand. Bangkok: Faculty of Applied Science, KMUTNB; 2017 [cited 2017 Oct 10]; 129–133.
[14] Mateos-Aparicio I, Redondo-Cuenca A, Villanueva-Suárez MJ. Isolation and characterization of cell wall polysaccharides from legume by-products: Okara (soymilk residue), pea pod and broad bean pod. Food Chem 2010;122:339–45.
[15] Kanlayavattanakul M, Lourith N, Chaikul P. Jasmine rice panicle: A safe and efficient natural ingredient for skin aging treatments. J Ethnopharmacol 2016;193:607–16.
[16] Oyarzun-Ampuero FA, Brea J, Loza MI, Torres D, Alonso MJ. Chitosan–hyaluronic acid nanoparticles loaded with heparin for the treatment of asthma. Int J Pharm 2009;381:122–9.

[17] De la Fuente M, Seijo B, Alonso MJ. Novel hyaluronic acid-chitosan nanoparticles for ocular gene therapy Invest Ophthalmol Vis. Sci 2008;49:2016–24.
[18] Lademann J, Richter H, Teichmann A, et al. Nanoparticles–an efficient carrier for drug delivery into the hair follicles. Eur J Pharm Biopharm 2007;66:159–64.
[19] Alvarez-Román R, Naik A, Kalia YN, Guy RH, Fessi H. Skin penetration and distribution of polymeric nanoparticles. J Control Release 2004;99:53–62.
[20] Crini G. A history of cyclodextrins. Chem Rev 2014;114(21):10940–75.
[21] Charlot A, Heyraud A, Guenot P, Rinaudo M, Auzély-Velty R. Controlled synthesis and inclusion ability of a hyaluronic acid derivative bearing β-cyclodextrin molecules. Biomacromolecules 2006;7:907–13.
[22] Sivasubramanian M, Park JH. Synthesis and characterization of hyaluronic acid-α-Cyclodextrin conjugate as the potential carrier of PEGylated drugs. J Pharm Investig 2010;40:219–23.
[23] Yin H, Zhao F, Zhang D, Li J. Hyaluronic acid conjugated β-cyclodextrin-oligoethylenimine star polymer for CD44-targeted gene delivery. Int J Pharm 2015;483:169–79.
[24] De la Fuente M, Seijo B, Alonso MJ. Bioadhesive hyaluronan–chitosan nanoparticles can transport genes across the ocular mucosa and transfect ocular tissue. Gene Ther 2008;15:668–76.
[25] Baysal K, Aroguz AZ, Adiguzel Z, Baysal BM. Chitosan/alginate crosslinked hydrogels: Preparation, characterization, and application for cell growth purposes. Int J Biol Macromol 2013;59:342–8.
[26] Cowman MK, Matsuoka S. Experimental approaches to hyaluronan structure. Carbohydr Res 2005;340:791–809.
[27] Takayama K, Hirata M, Machida Y, Masada T, Sannant T, Nagai T. Effect of interpolymer complex formation on bioadhesive property and drug release phenomenon of compressed tablet consisting of chitosan and sodium hyaluronate. Chem Pharm Bull 1990;38:1993–7.
[28] Necas J, Bartosikova L, Brauner P, Kolar J. Hyaluronic acid (hyaluronan): a review. Vet Med. 2008;53:397–411.
[29] Raju MP, Raju KM. Design and synthesis of superabsorbent polymers. J Appl Polym Sci 2001;80:2635–9.
[30] Kanlayavattanakul M, Lourith N, Tadtong S, Jongrungruangchok S. Rice panicles: New promising unconventional cereal product for health benefits. J Cereal Sci 2015;66:10–17.
[31] Monnery BD, Wright M, Cavill R, et al. Cytotoxicity of polycations: Relationship of molecular weight and the hydrolytic theory of the mechanism of toxicity. Int J Pharm 2017;521:249–58.